Journal of Cleaner Production 255 (2020) 120178

Contents lists available at ScienceDirect

Journal of Cleaner Production

journal homepage: www.elsevier.com/locate/jclepro

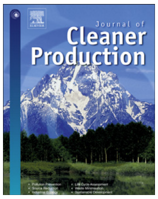

Zero-waste process for the transformation of a hazardous aluminum waste into a raw material to obtain zeolites

Aurora López-Delgado [a], [*], José I. Robla [a], Isabel Padilla [a], Sol López-Andrés [b], Maximina Romero [c]

[a] National Center for Metallurgical Research, CSIC, Av. Gregorio del Amo 8, Madrid, 28040, Spain
[b] Faculty of Geology, Universidad Complutense de Madrid, Av. José Antonio Novais, Madrid, 28040, Spain
[c] Eduardo Torroja Institute for Construction Sciences, CSIC, C/ Serrano Galvache 4, Madrid, 28033, Spain

ARTICLE INFO

Article history:
Received 27 September 2019
Received in revised form
19 December 2019
Accepted 16 January 2020
Available online 25 January 2020

Handling Editor: M.T. Moreira

Keywords:
Zero-waste process
Hazardous aluminum waste
Pilot-scale
Zeolite A

ABSTRACT

A potential route to minimize the environmental impact of industrial activities is, among other approaches, the use of hazardous wastes as less-common raw materials for the preparation of other materials. Realistic technologies for waste management should include simple and low-cost processes as well as the nonproduction of new wastes. Thus, the total conversion of a type of hazardous aluminum waste into zeolite was achieved at the pilot-scale (200 l autoclave reactor) under mild hydrothermal operating conditions. In a one-step process, 3.2 tons of zeolite, 76.4 Nm^3 of ammonia and 105.9 Nm^3 of hydrogen can be produced per ton of aluminum waste. The process does not generate other wastes. The recycling of process effluents (mother liquor and rinse water), along with the process gases capture and its subsequent commercialization, would increase the environmental impact and the economic yield. The obtained Linde type-A zeolite, exhibited structural, textural and morphological characteristics similar to those of zeolites prepared from commercial reagents. A conceptual design for zero-waste process is proposed. The sustainable process developed can contribute to reduce the high environmental impact of aluminum industry waste, and contribute to the circular economy by converting a hazardous waste into a raw material.

1. Introduction

The increase in hazardous waste generation, associated with rapid global industrialization, has become a relevant environmental problem (Gautam et al., 2016). The development of more sustainable processes that alleviate such environmental impacts is absolutely necessary. Using hazardous wastes as less-common raw materials for the preparation of valuable materials must be considered as a potential alternative to minimize waste generation and management (López-Delgado and Tayibi, 2012). Moreover, hazardous wastes require a chemical pretreatment prior to being disposed of in landfills, with a consequent increase of the management cost (Anuwattana and Khummongkol, 2009). In addition, public policy approaches, based on the zero-waste concept, aim to minimize the negative effects of the generation and management of waste on human health and the environment, as well as to reduce the use of resources (European_Directive-2008/98/EC, 2008).

Among hazardous wastes, aluminum wastes can lead to negative impacts on the environment due to their very fine grain sizes and multiphase compositions containing harmful substances (Renda et al., 2013). Globally, aluminum is one of the most widely used metals. The world production of aluminum was approximately 63.4 million tons in 2017 and the global consumption of this metal is estimated to exceed 100 million tons in 2025 (IAI, 2018).

This metal is obtained from bauxite in the primary industry and from materials that have reached the end of their life (scraps) in the secondary industry (Osoba et al., 2018). Both industries generate wastes, in particular slag or dross, which are recycled by the tertiary industry by means of shredding, milling, and sieving processes, followed by granulometric classification (Galindo et al., 2015; Huang et al., 2014, 2015; Mahinroosta and Allahverdi, 2018).

The different treatments, including recovery and/or disposal operations, of hazardous wastes from industrial activities are regulated

---

[*] Corresponding author.

E-mail addresses: alopezdelgado@cenim.csic.es (A. López-Delgado), jrobla@cenim.csic.es (J.I. Robla), isapadilla@cenim.csic.es (I. Padilla), antares@ucm.es (S. López-Andrés), mromero@ietcc.csic.es (M. Romero).

https://doi.org/10.1016/j.jclepro.2020.120178
0959-6526/

through the Directive 2008/98/EC of the European Parliament and the European Waste Catalogue (EWC) (European_Directive-2008/98/EC, 2008). According to this list, the majority of hazardous wastes from aluminum metallurgy are represented by primary smelting slag (code 100304), salt slag from secondary smelting (code 100308), black dross from secondary smelting (code 100309), and other particulates and dust (including ball mill dust) containing hazardous substances (code 100321). The last type of waste, hereinafter referred to as AlW, is considered to be: "highly flammable" (H3-A), "harmful": (H5), "able to release toxic gases" (H12) and "leachable" (H13). The main negative impacts of AlW come from its very fine grain size and its heterogeneous chemical and mineralogical composition containing harmful substances such as metallic aluminum, aluminum nitride, aluminum carbide, aluminum sulfide, and heavy metals. Additionally, AlW can react with water or humidity generating certain toxic gases, such as ammonia, methane and hydrogen sulfide, and/or inflammable and explosive gases like hydrogen (Osoba et al., 2018).

Spain has a large industrial aluminum sector, although very fragmented in many medium and small companies, including primary production (as the third largest producer in Europe) as well as secondary and waste recycling. The production of AlW is approximately 16,000 t/year, and it is generally disposed into secure landfills, i.e., it is not recovered (Sánchez-Hernández, 2018).

The total aluminum content in AlW is distributed among different compounds, principally Al_2O_3, AlN, Al°, and Al_2MgO_4 which yield a total percentage ranging from 53 to 81% in weigh (expressed as oxide) (Galindo et al., 2015). In addition, AlW contains SiO_2 ranging between 3 and 18 wt% and different metal oxides (Fe, Cu, etc) along with alkaline salts. Taking into account the mineralogical and chemical composition of the AlW and, the zero-waste concept, its use as a raw material for the synthesis of zeolite was recently envisaged as a useful and advantageous option for its management. In this context, NaP1, analcime and sodalite zeolites were obtained by a simple laboratory-scale synthesis route by means of varying the synthesis parameters such as crystallization temperature and alkaline agent concentration (Sánchez-Hernández, 2018; Sánchez-Hernández et al., 2016, 2017).

In a huge effort to attain cleaner and eco-efficient processes for the production of zeolites, different wastes or byproducts have been studied as raw materials. (Veeresh P. Mallapur and Oubagaranadin, 2017; Zhang and Li, 2018). The synthesis of zeolite-like materials from wastes has been accomplished mostly by using fly ash because it exhibits a chemical structure similar to that of zeolite, with high SiO_2 content and low Al_2O_3 content (Álvarez-Ayuso et al., 2003; Cardoso et al., 2015; Chareonpanich et al., 2011; Querol et al., 2001, 2002). Some of the disadvantages of the use of fly ash to produce zeolite are the low yield of the process and, the need for several stages, to eliminate the carbonaceous material (Anuwattana and Khummongkol, 2009; Terzano et al., 2015).

Compared to using fly ash, the main novelty of the use of AlW as a raw material for the synthesis of zeolite comes from its totally different chemical composition. In fly ash, the chemical structure of the zeolite is inferred. However, in AlW the content of Al_2O_3 is much higher and the content of SiO_2 is much lower than that of fly ash. In addition, the total aluminum content of AlW, which is presented as different mineralogical phases (metallic aluminum, aluminum nitride, spinel, corundum, etc.) is used to form the zeolite framework, so that the transformation of aluminum waste is completed without generation of other solid waste (Sánchez-Hernández et al., 2016). Concerning other aluminum wastes, Terzano et al. (2015) described the use of glass and aluminum cans from the Municipal Solid Waste System to obtain a zeolitic material with approximately 30% of zeolite A, by a long thermal process (one week, 60 °C) at laboratory-scale. Anuwattana et al. (Anuwattana and Khummongkol, 2009) described the synthesis of Na-A zeolite from cupola slag and an aluminum sludge from an aluminum plating plant. The laboratory-scale process involved the pretreatment of the wastes by magnetic separation, calcination and alkaline fusion at 700 °C.

The present work is focused on achieving the complete transformation of a type of hazardous aluminum waste into a zeolite at pilot-scale, prior to industrial process implementation. This proposed process, based on the authors' previous experiences (Sánchez-Hernández et al., 2016, 2017), consists of a hydrothermal process carried out in only one step and under mild operating conditions. The mineralogical, structural and morphological characterization of the obtained zeolite was performed mainly by X-ray diffraction (XRD), infrared spectroscopy (FTIR) and scanning electron microscopy (SEM). The thermal behavior analyzed by TG/DTA, and the textural characteristics of the zeolite, including the specific surface area (S_{BET}), pore volume and pore size distribution, were also determined. In addition, a conceptual flow diagram designed for the complete valorization of the hazardous waste by means of its transformation into zeolite is presented. The process also included the recovery of the generated gases (ammonia and hydrogen) as byproducts.

2. Materials and methods

2.1. Materials

The aluminum waste (AlW) used for the synthesis of zeolite at the pilot-scale comes from the tertiary aluminum industry; indeed, it is the finest grain fraction of aluminum slag milling, which is collected by sleeve filters. As mentioned above, AlW is a hazardous waste included in the European Waste Catalogue with the reference code 100321. The chemical composition of the waste consists of about 77 wt% aluminum (expressed as Al_2O_3) and 4 wt% SiO_2, according to the X-Ray Fluorescence (XRF) analysis, as shown in Table 1. The total aluminum content is distributed among different compounds such as, metallic aluminum, aluminum nitride (AlN), corundum (Al_2O_3), and spinel ($MgAl_2O_4$). The sodium, potassium and chloride contents are attributable to the use of high amounts of salt in the aluminum scrap melting process. The content of TiO_2 (~5 wt%), which is associated with different types of scrap used for producing aluminum ingots, was noticeable. These values are within the normal values found for this type of waste (Galindo et al., 2015). This hazardous waste is a smelly, dark gray powder characterized by high reactivity in the presence of humidity (H5, H12), as a consequence of its high aluminum nitride (14 wt%) and metallic aluminum (8.5 wt%) content. Thus, AlW can generate toxic and inflammable gases such as ammonia and hydrogen according to reactions 1 and 2, respectively (Sánchez-Hernández, 2018):

$$2AlN + 3H_2O \rightarrow 2NH_3(g) + Al_2O_3 \quad \Delta G^0_{25^\circ C} = -327,92\ kJ \tag{1}$$

$$2Al + 3H_2O \rightarrow 3H_2(g) + Al_2O_3 \quad \Delta G^0_{25^\circ C} = -866,67\ kJ \tag{2}$$

Table 1
Main chemical composition of the aluminum waste (expressed as wt.%) determined by X-ray fluorescence (XRF).

Al_2O_3	SiO_2	MgO	TiO_2	K_2O	CaO	Cl^-	Na_2O	Others	AlN[a]	Al[b]
77.14	3.96	3.10	4.55	4.38	1.73	1.85	1.10	2.19	14.10	8.52

[a] Content of aluminum nitride determined by the Kjeldahl method.

[b] Content of metallic aluminum determined by atomic absorption spectroscopy (AAS).

A commercial sodium silicate solution, (waterglass $3.3SiO_2 \cdot Na_2O$, pH = 12.5, $\rho = 1.35$ g cm^{-3}) was used to increase the low Si/Al ratio of the waste. Sodium hydroxide solution was prepared by dissolving NaOH pellets in tap water. This type of water was also used as process water and for washing the zeolite obtained in the process.

2.2. Pilot-scale synthesis

The pilot-scale synthesis was performed in a one-step hydrothermal process under mild operating conditions, to evaluate the feasibility of using AlW as a raw material to achieve a zeolite at the industrial scale. The hydrothermal synthesis process was carried out employing a 200 l stainless steel autoclave reactor (Fig. 1a), which was equipped with an agitation system (power of 4 kW). The reactor was loaded with approximately 10 kg of aluminum waste, 5.3 kg of NaOH pellets, 22.9 kg of waterglass and 132 l of tap water. The reaction was maintained with continuous stirring and under autogenous pressure of 1 bar, at 80 °C for 12 h. After the reaction time, the product was discharged by a valve located at the bottom of the reactor; the solid was separated from its mother liquor by filtration using a 50 l and 37 cm diameter stainless steel pressure filter, at a working pressure of 4.5 bar (Fig. 1b).

To avoid gas generation inside the reactor (see eqs. (1) and (2)), the aluminum waste was partially hydrolyzed with water and NaOH solution. Then, it was loaded along with the rest of the reactants by a valve located on the top of the reactor. Fig. 2 shows an image of the AlW during the hydrolysis step. First, small bubbles were formed (Fig. 2a), but as the hydrolysis of aluminum nitride proceeded, very large bubbles were observed due to the emission of ammonia (Fig. 2b). Although the gases evolved were not recovered in this trial, because of the lack of an appropriate gas installation, their recovery as byproducts is considered in the conceptual design presented below.

The filtration of the reaction product was performed in batches and the filter cakes were rinsed twice with tap water using the same pressure filter (Fig. 3). The humidity of the as-obtained filter cake was 30 wt%. Later, the filter cake was dried at 100 °C until a constant mass value was attained.

2.3. Characterization techniques

The chemical composition of the AlW was determined by X-ray fluorescence (XRF), using a wavelength dispersive X-ray fluorescence spectrometer (Bruker, S8 Tiger), with a rhodium anode and 4 kW excitation power. Measurements were performed on a fusion disk prepared with lithium tetraborate and lithium metaborate with tube settings of 60 kV and 170 mA using LiF (220), LiF (200), PET, and XS-55 as analyzer crystals. The content of aluminum nitride in the hazardous waste was analyzed by the Kjeldahl method using an automatic steam distilling unit (UDK 130 A, Velp Scientifica), and subsequent titration of the resulting solution with a standardized 1 M HCl solution. The content of metallic aluminum was determined by treating the sample with a 10% HCl solution to dissolve aluminum, which was analyzed in the filtrate by atomic absorption spectrometry (AAS) in a Varian Spectra model AA-220FS equipment. Mineralogical characterization of zeolite was performed by X-ray diffraction (XRD) using a Bruker D8 Advance

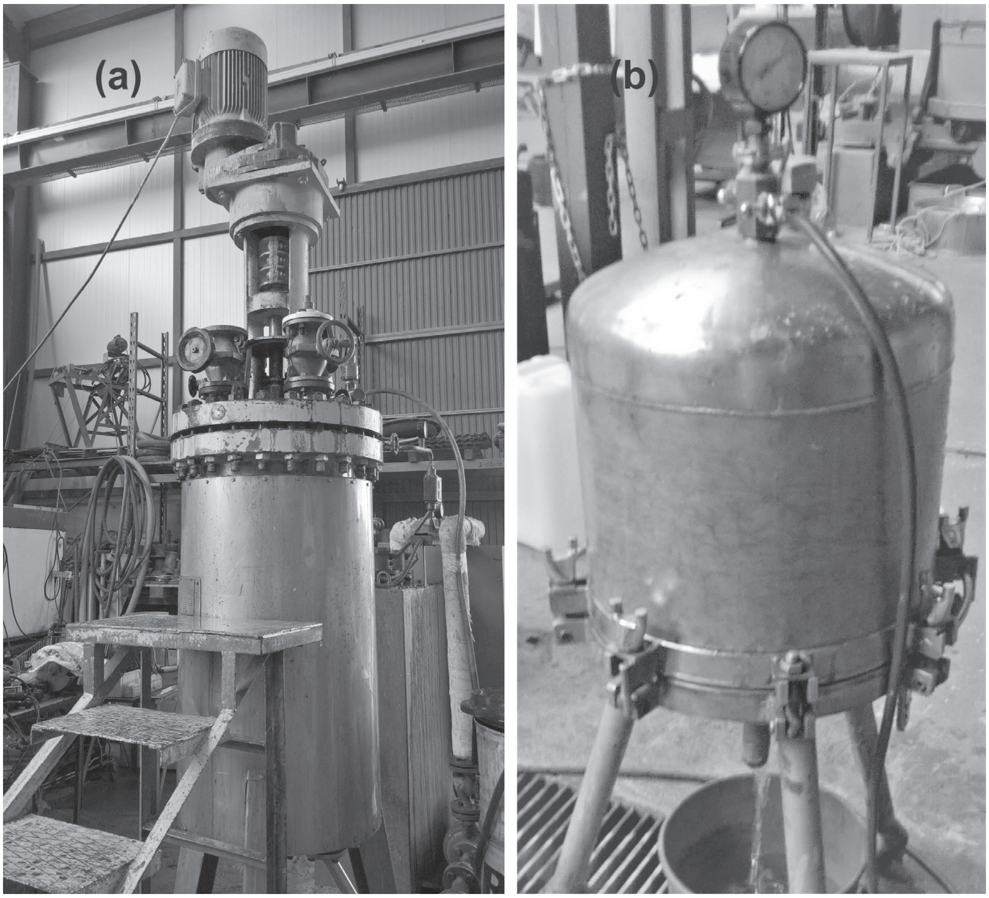

Fig. 1. (a) Autoclave reactor (200 l) used for the synthesis of zeolite from the aluminum waste and (b) pressure filter used for the separation of the zeolite from its mother liquor.

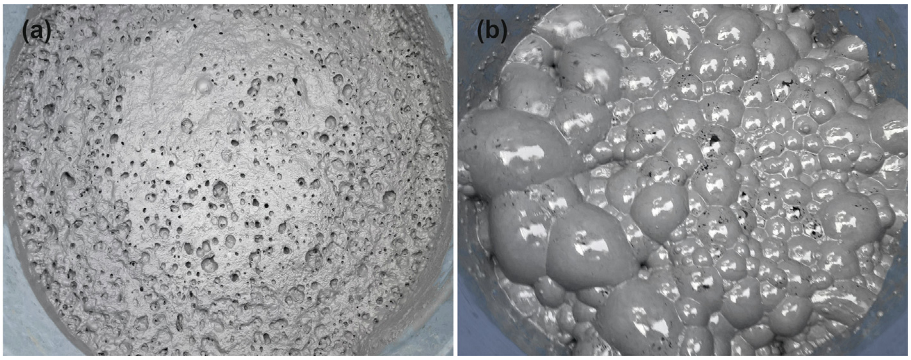

Fig. 2. Gas generation during the hydrolysis of AlW with a NaOH solution.

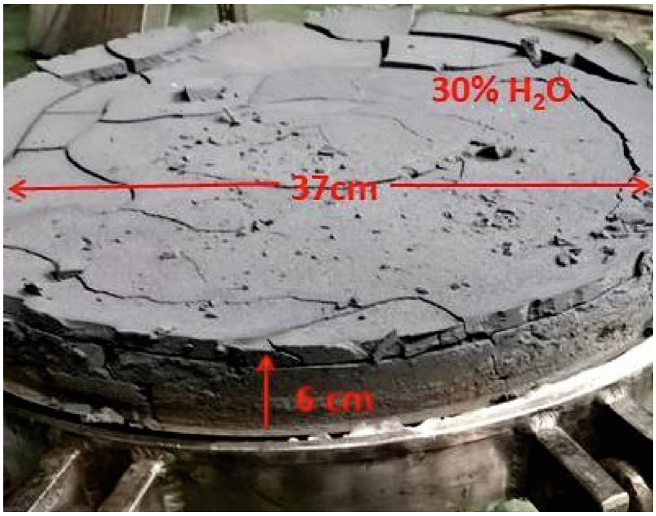

Fig. 3. Aspect of the zeolite filter cake obtained by batch pressure filtration.

Diffractometer with CuKα radiation, with 2θ from 5° to 60°, at a scan rate 2θ of 0.02°, 5 s per step. Tube settings were 40 kV and 30 mA. The semiquantification of the crystalline phases was performed using EVA software. The morphology and composition were determined by field emission scanning electron microscopy (FE-SEM), using a Hitachi S4800 microscope (5.0 kV, 10.0 mm), equipped with an energy-dispersive X-ray spectroscopy (EDS) detector for semi-quantitative analysis. Before the FE-SEM observations, the sample was coated with graphite by a sputtering procedure. The Fourier transform infrared (FTIR) spectrum of the zeolite was recorded on KBr discs (Nicolet Nexus 670–870) in the range of 400–1300 cm^{-1}. Textural characterization of the zeolite was performed by determination of nitrogen adsorption/desorption isotherms at 77 K in an ASAP 2010 Micromeritics system. The sample was previously outgassed at 250 °C in vacuum for 24 h. The specific surface area (S_{BET}) was calculated by the BET method in the P/Po range of 0.002–0.3. The external area (S_{Ext}), i.e., the area of those pores that are not micropores (mesopores, macropores, and the exterior surface of the particle), was calculated by the t-plot method from the slope of the linear fit in the thickness range (t) of 0.35–0.5 nm according to the Harkins-Jura equation. The pore size distribution was calculated using the Barrett-Joyner-Halenda (BJH) method in the desorption branch of the isotherm. The thermal behavior of the zeolite was studied from room temperature to 1000 °C by thermogravimetric and differential thermal analysis (TG/DTA), in a SETARAM Labsys thermal analyser (heating rate of 10 °C/min under an air flow of 100 ml/min).

3. Results and discussion

The macroscopic appearance of the product obtained at the pilot-scale corresponds to a homogeneous fine grain solid with a very clear gray color as shown in the image (Fig. 4a). The total amount of dried solid obtained in the process was 32 kg. The XRD pattern of this sample is shown in Fig. 4b. The diffraction profile can be assigned to that corresponding to zeolite A, which is one of the synthetic aluminosilicates classified under the Linde type framework (LTA-zeolites) (Ayele et al., 2016). This XRD pattern has been indexed according to the hkl indexes reported by (Hashemian et al., 2013) for this type of zeolite prepared from chemical reagents (sodium aluminate and sodium metasilicate) at 100 °C for 24 h. Similar patterns are reported for zeolite A synthesized at the laboratory scale from K-feldspar at 90 °C for 12 h with a previous treatment of the raw materials at 280 °C (Su et al., 2016) and from fly ash by alkaline fusion (900 °C), prior to hydrothermal treatment (Volli and Purkait, 2015).

The experimental interplanar distances, d values in Å, and those corresponding to the ICDD PDF reference database are listed in Table 2. The reference file 01-073-2340 corresponds to a synthetic LTA zeolite with stoichiometry $Na_{12}Al_{12}Si_{12}O_{48}(H_2O)_{27}$, space group Fm-3c, a cubic crystal system and a cell parameter a = 24.6100 Å, fitting well to the experimental values of zeolite from aluminum waste, a = 24.583 Å. The crystallite size calculated by Scherrer equation was 36.2 nm; and the semiquantification of the crystalline phases yielded 93.8 wt% zeolitic material and 6.2 wt% corundum.

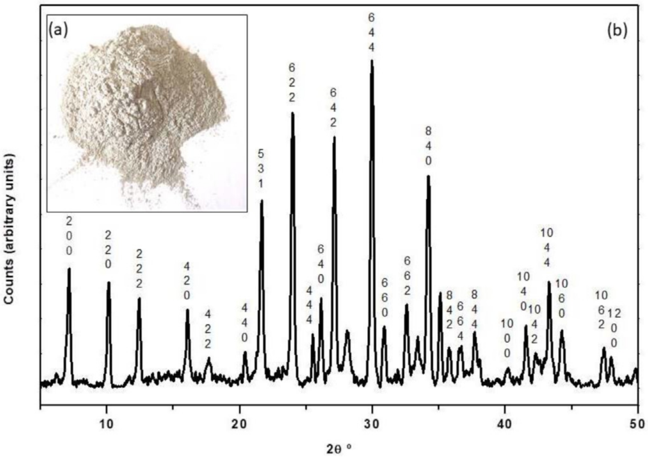

Fig. 4. Macroscopic appearance (a) and XRD pattern (b) of LTA zeolite obtained from AlW in a pilot-scale synthesis process under mild conditions.

The SEM image of the obtained zeolite is shown in Fig. 5a, in which a typical cubic crystal with homogeneous size distribution is observed. This is a characteristic morphology of zeolite A (Anuwattana and Khummongkol, 2009; Ayele et al., 2015, 2016; Ismail et al., 2010) with both shape and size highly dependent on the Na_2O:Al_2O_3:SiO_2 ratio. Radulović et al. (2013) reported the presence of small agglomerates on the surface of the cubic crystal grains, especially for Na-LTA zeolite prepared under hydrothermal conditions from sodium silicate and sodium aluminate solutions at 90 °C, with an excess of SiO_2 in relation to the ideal stoichiometry Al_2O_3:$2SiO_2$. The EDS analysis of the obtained zeolite revealed the following average composition (% atom): Na = 8.8, Al = 10.3, Si = 12.3 and K = 0.6. The presence of potassium came from the initial composition of the waste, and this cation most likely replaces sodium ions in the zeolite structure. Na^+ is the principal exchange cation to stabilize the structure of the Linde-type A zeolite, but the charge is balanced by the presence of K^+ (Sánchez-Hernández et al., 2016). The average Si/Al ratio performed by EDS analysis is 1.19 (consistent with the excess waterglass added in the autoclave reactor), which is characteristic of low-silica zeolites such as zeolite A. The (Na + K)/Al ratio is 0.92, which fits well with the typical stoichiometric value for this type of zeolite with the ideal formula of $NaAlSiO_4$ (Kugbe et al., 2009). Fig. 5b shows the framework-structure of zeolite A composed of double 4-rings (IZA, 2017; Xu et al., 2007).

Fig. 6 shows the FTIR spectrum of the zeolite recorded from 1200 to 400 cm^{-1}, This is the region in which the fundamental vibrations of the framework $(Si,Al)O_4$ tetrahedra appear. Two types of vibrations are observed in this zone for zeolites: the internal vibrations of the framework tetrahedron, and vibrations related to external linkages between tetrahedra (secondary building units) (Flanigen et al., 1974). The FTIR spectrum of the zeolite obtained from the AlW is characteristic of zeolite A: a very strong band at 1006 cm^{-1} corresponds to the asymmetric stretching vibrational mode, and a weak band at 668 cm^{-1} corresponds to the symmetric stretching vibrational mode. These bands along with the bending mode at 463 cm^{-1} (medium intensity) are due to the internal vibrations of the tetrahedra. The medium strong band at 560 cm^{-1} corresponds to the vibrations of the secondary building units (double 4-rings) (Flanigen et al., 1974). Similar values of FTIR bands are reported for both commercial zeolite 4A and zeolite synthesized from kaolin (Wang et al., 2019).

Table 2
Experimental d values from the XRD pattern and reference file ICDD 01-073-2340.

d_{exp} (Å)	$d_{01\text{-}073\text{-}2340}$ (Å)	hkl
12.252	12.305	2 0 0
8.709	8.700	2 2 0
7.092	7.104	2 2 2
5.499	5.502	4 2 0
4.994	5.023	4 2 2
4.352	4.350	4 4 0
4.166	4.159	5 3 1
3.704	3.710	6 2 2
3.545	3.552	4 4 4
3.410	3.412	6 4 0
3.280	3.288	6 4 2
2.987	2.984	6 4 4
2.903	2.900	6 6 0
2.819	2.822	6 6 2
2.754	2.751	8 4 0
2.683	2.685	8 4 2
2.620	2.623	6 6 4
2.508	2.511	8 4 4
2.457	2.461	10 0 0
2.285	2.284	10 4 0
2.239	2.246	10 4 2
2.142	2.142	10 4 4
2.107	2.110	10 6 0
2.079	2.079	10 6 2
2.048	2.050	12 0 0

According to the XRD, SEM and FTIR studies, the as-obtained zeolite exhibits crystalline, structural and morphological characteristics similar to those of zeolites prepared from both commercial reagents (Hashemian et al., 2013; Kugbe et al., 2009; Radulović et al., 2013) and other types of wastes (Anuwattana and Khummongkol, 2009; Ayele et al., 2015, 2016; Chareonpanich et al., 2011; Wang et al., 2019).

The nitrogen adsorption-desorption isotherms of the obtained zeolite are shown in Fig. 7a. According to IUPAC, the isotherm is classified as type II, which is characteristic of mesoporous materials with a certain number of micropores. Hysteresis loop for this zeolite is classified as H3. The abrupt closure of the hysteresis loop at a relative pressure P/P° of 0.45 is due to the breakage of the liquid nitrogen meniscus at this relative pressure followed by emptying of the pores. Similar results were reported for zeolite A obtained from fly ash (Volli and Purkait, 2015) and from kaolin (Wang et al., 2019). The external area surface was 7.7 m^2/g and the surface calculated by the use of the BET equation was 19.7 m^2/g; the difference between these values gives a relatively high micropore area of 12 m^2/g. The micropore volume obtained was 0.006 cm^3/g. Fig. 7b indicates that the dominant pore diameter is located at 3.8 nm. BET surface values of 13.37 and 7.37 m^2/g are reported for synthesized and commercial zeolite 4A, respectively (Wang et al., 2019).

TG/DTA curves for the zeolite are plotted in Fig. 8. The mass loss (approximately 4 wt %) observed in the TG plot up to 230 °C corresponds to the dehydration of zeolite. This process occurs in two different steps according to the DTA curve, in which two endothermic peaks centered at 97 °C and 141 °C can be observed. Dehydrated zeolite lattices is stable at high temperature (up to 850 °C), and then conversion of the LTA zeolite into nepheline occurs by solid-solid topotactic transformation (Dimitrijevic et al., 2004). Thus the exothermic peak centered at 890 °C observed in the DTA plot, is attributable to the formation of nepheline from the LTA zeolite framework. The XRD pattern of this phase (Fig. 8) fit well with the reference file ICDD 01-083-2372 corresponding to the hexagonal nepheline phase.

One of the problems associated with the use of wastes as raw materials for the synthesis of zeolite, comes from the need for a developing process with multiple steps, negatively affecting both the realistic application of the process on an industrial scale and the process yield. Simple and low-cost processes are desirable to minimize the cost of the production of zeolite and, accordingly, the challenge of valorizing the waste. (Anuwattana and Khummongkol, 2009; Baccouche et al., 1998; Farag and Zhang, 2012; Wang et al., 2008; Wdowin et al., 2014; Yang and Yang, 1998). The advantages of the presented process to obtain zeolite from AlW are as follows:

a) The zeolite is obtained in a single step and only a synthesis reactor is required; accordingly the process could be easily scaled. Table 3 presents a comparative study of several synthesis processes to obtain zeolite A from different raw materials. All processes to obtain zeolite A from different wastes required multiple steps, including the pretreatment of those wastes.

b) The reaction yield is very high because the waste is entirely transformed into a zeolitic material Thus, 3.2 kg of zeolite can be obtained per kg of aluminum waste. Because no other solids are formed, it can be considered that the aluminum waste has been completely transformed into a zeolite (yld = 100%). The yield reported in other studies is very low; i.e.; 85 g of zeolite per kg of carbon fly ash was reported by

Table 3
Synthesis conditions of zeolite A from different raw materials.

Raw materials	Raw material Pretreatment	Hydrothermal treatment for zeolitization	Scale	References
Cupola slag and aluminum sludge	Grounding/sieving and acid treatment, calcination at 700 °C of cupola slag Acid washing, alkaline fusion at 700 °C for aluminum sludge.	90 °C, 9 h	laboratory	Anuwattana and Khummongkol (2009)
Kaolin	Metakaolinization 600-700 °C, 2–3 h	70-200 °C 24–120 h	laboratory	Johnson and Arshad (2014)
Coal fly ash and aluminum metal powder	Activation of fly ash at 100 °C, 24 h Dissolution of aluminum metal powder	95 °C, 4 h	laboratory	Cardoso et al. (2015a)
Subbituminous coal fly ash and bottom ash	Reflux acid treatment, alkaline fusion 900 °C, 1 h	120 °C, 4 h	bench	Chareonpanich et al. (2011)
Fly ash	Alkaline treatment 90 °C, 24 h	90 °C, 48 h	bench	Hollman et al. (1999)
Glass and aluminum from MSW	Dissolution of glass Dissolution of aluminum pieces in alkaline medium	60 °C, 7 days	laboratory	Terzano et al. (2015)
This paper	Not required	80 °C, 12 h	pilot	

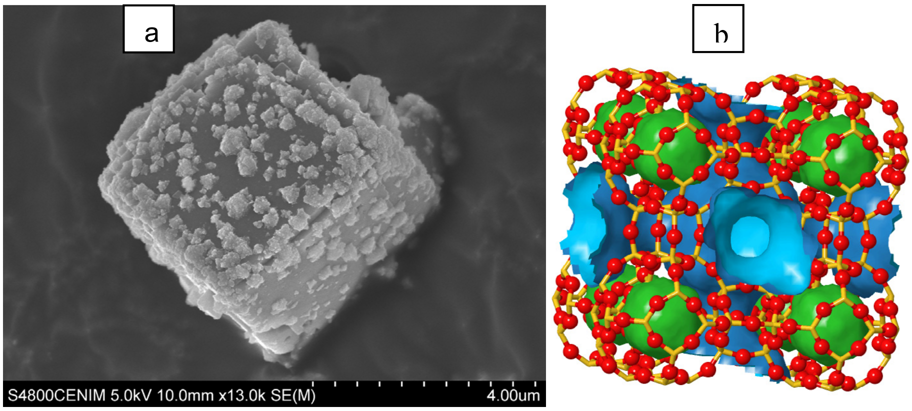

Fig. 5. SEM image of a cubic crystal grain of the zeolite obtained at the pilot-scale from AlW (a). Framework of zeolite A. The 3-dimensional channel system and cages are represented in blue and green, respectively (b) (IZA, 2017).

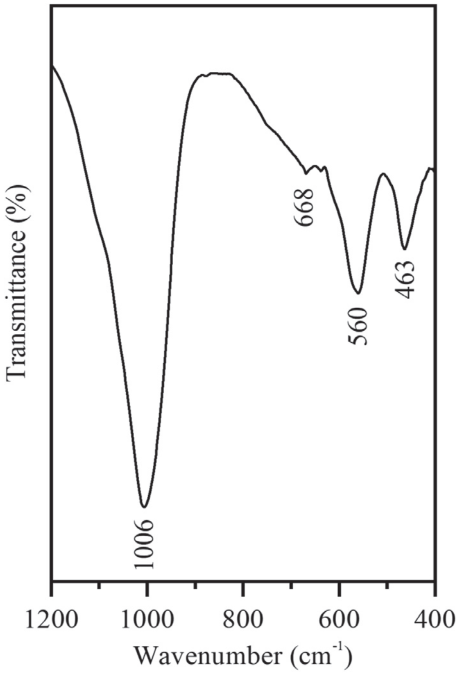

Fig. 6. FTIR spectrum of zeolite A obtained from AlW at the pilot-scale.

(Hollman et al., 1999) (yld = 8.5%), and Sommerville et al. (2013) reported yield reaching 250 g/kg fly ash (yld = 25%)

c) Marketable gases such as hydrogen and ammonia are collected as valuable byproducts. In total, 76.4 Nm^3 of NH $_3$ and 105.9 Nm^3 of H_2 can be recovered per ton of AlW.
d) The industrial-scale process should be considered as a low-cost process because the required installation is very simple and complex design is not required.
e) By using a waste as a raw material, the disposal cost (approximately 110 €/t) is saved. The disposal cost increases because hazardous waste should be pretreated prior to its acceptance in a landfill according to environmental policies (Anuwattana and Khummongkol, 2009).
f) An environmental benefit is obtained with the use of a waste as a raw material. Thus, the higher the amount of hazardous waste is to be disposed of in a landfill, the higher the need to acquire new natural spaces to increase the size of the landfill or to build new ones.

A conceptual flowsheet of the process for the manufacturing of different types of zeolites from AlW is shown in Fig. 9.

Raw materials (AlW, NaOH, waterglass and water) are charged into the autoclave reactor, equipped by an agitation system and a steam generator for indirect heating.

Because of the composition of the AlW, the next stages and reactions can be considered up to the zeolite formation:

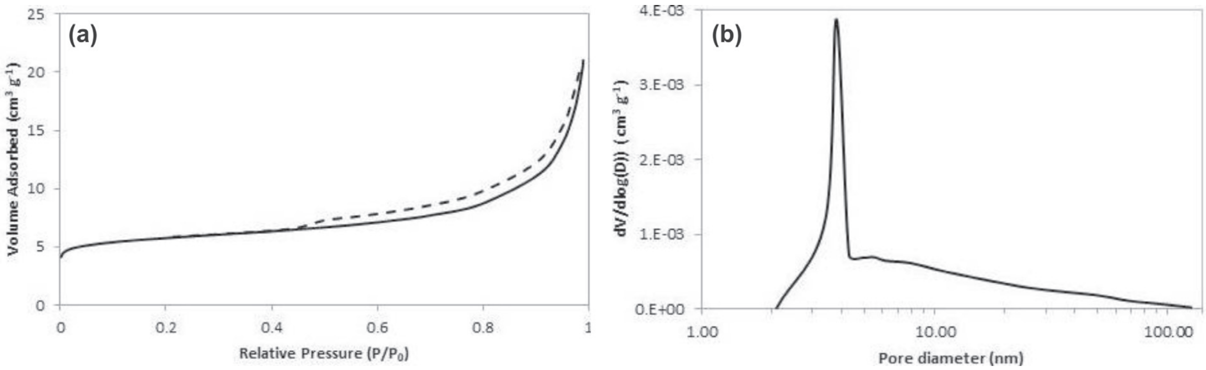

Fig. 7. Nitrogen adsorption-desorption isotherm (a) and distribution of the pore diameter (b) of zeolite A obtained at the pilot-scale from AlW.

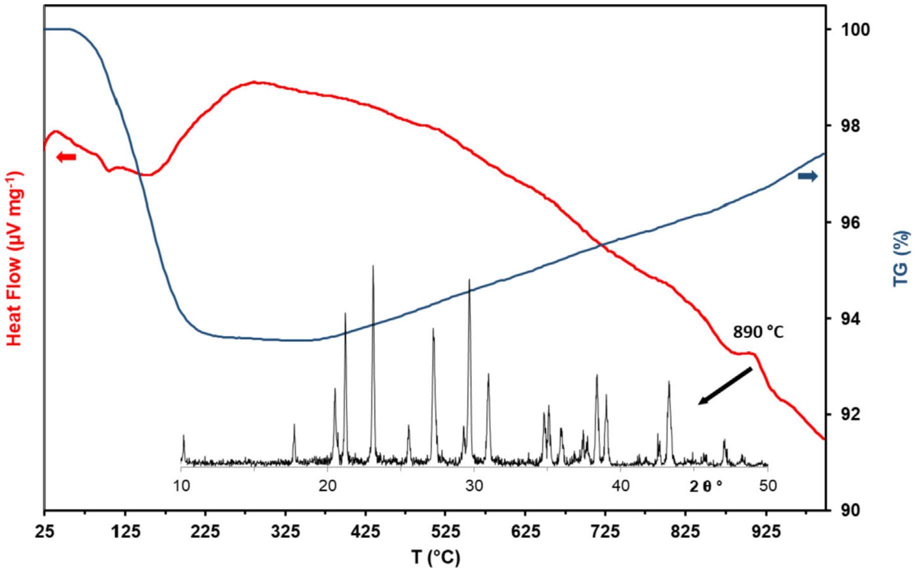

Fig. 8. TG/DTA curves of the zeolite obtained from AlW along with the XRD pattern of nepheline (ICDD 01-083-2372).

1. Hydrolysis of different aluminum compounds in the AlW, principally metallic aluminum and aluminum nitride according to equations (3) and (4), respectively and the subsequent formation of AlO_2^- ions as the pH value increases.

$$2Al + 2OH^- + 2H_2O \rightarrow 2AlO_2^- + 3H_2 \tag{3}$$

$$AlN + OH^- + H_2O \rightarrow AlO_2^- + NH_3 \tag{4}$$

2. Dissolution of the aluminum oxide in the waste under alkaline conditions, according to equation (5).

$$Al_2O_3 + 2OH^- \rightarrow 2AlO_2^- + H_2O \tag{5}$$

3. Reaction of AlO_2^- ions with silicon polymer (waterglass) in the alkaline medium to form the corresponding zeolite. The formation of the zeolite occurs through a hydrogel route according to the literature (Bukhari et al., 2015; Farag and Zhang, 2012; Fawer et al., 1998).

$$NaAlO_2 + WG + 2NaOH \rightarrow Na\ Al\ SiO_4 \cdot nH_2O\ (\text{zeolite, gel}) \tag{6}$$

4. Final nucleation and crystal growth of zeolites by aging.

$$Na\ Al\ SiO_4 \cdot\ nH_2O\ (\text{zeolite, gel}) \rightarrow Na\ Al\ SiO_4\ (\text{LTA zeolite, dry}) \tag{7}$$

After the reaction period, the slurry is discharged from the reactor to a filter press to separate the zeolite from the mother liquor. In the same filter, the zeolite filter cake can be rinsed and the rinse water recycled to the reactor for a new process. Although a pressure filter was used in our experiment, we consider that a filter press is more adequate for an industrial process. Later, the zeolite filter cake was dried at 100 °C to obtain the dry powder.

Before the slurry discharge, the reactor is depressurized by opening the gas exit valve. The gas stream consists of a mixture of ammonia, hydrogen and water. Ammonia and hydrogen are considered valuable byproducts of the process. In the conceptual flowsheet a chemical process has been envisaged for the separation and valorization of both types of gases. Ammonia can be separated by blowing the gas stream throught a tartaric acid solution (Eq. (8)). Ammonium tartrate is precipitated and then, by heating, ammonia is collected separately (López-Delgado et al., 2017).

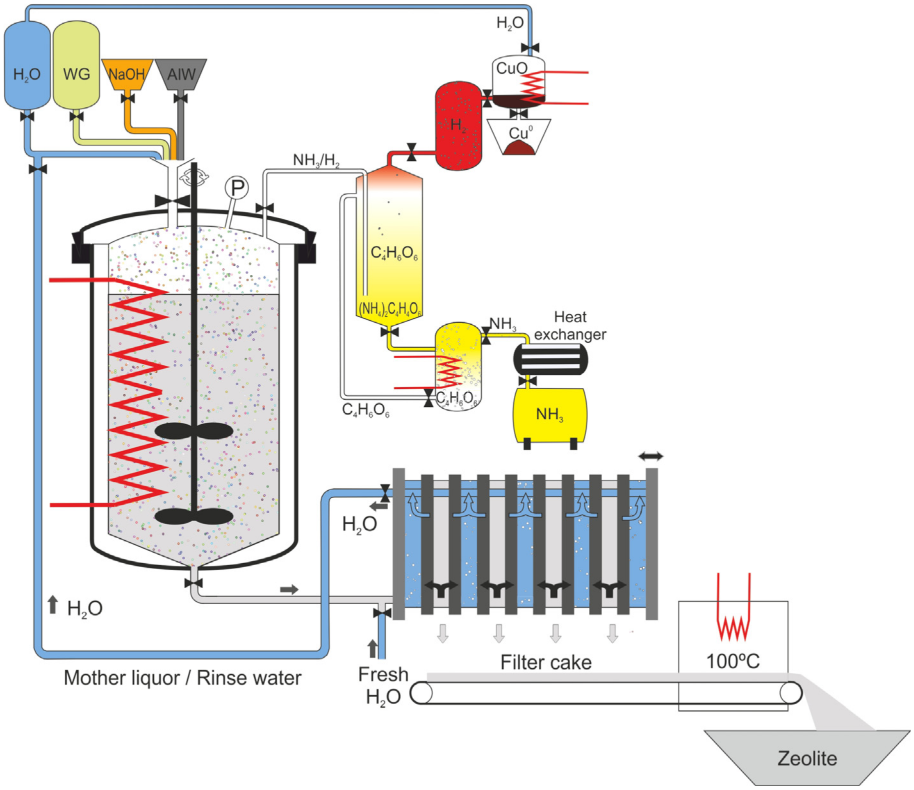

Fig. 9. Conceptual flowsheet for the manufacture of zeolite from AlW, with recovery of gases and effluent recycling.

$$C_2H_2(OH)_2(COOH)_2 + 2NH_4^+OH^- \rightarrow C_2H_2(OH)_2(COONH_4)_2 + 2H_2O \quad (8)$$

For the recovery of hydrogen, we propose an in situ metal oxide reduction, i.e., with CuO (Antrekowitsch, 2007; Arenas et al., 2019; Yamukyan et al., 2009) (Eq. (9)).

$$CuO + H_2 \rightarrow Cu + H_2O \quad (9)$$

For both gases and according to the aluminum and aluminum nitride contents in the AlW (Eqs. (1) and (2)), 76.4 Nm^3 NH_3 and 105.9 Nm^3 H_2 per ton of AlW can be achieved, respectively.

4. Conclusions

The described pilot-scale zeolitization process provides the total conversion of hazardous aluminum waste into an LTA zeolite. The reaction yielded approximately 3.2 tons of zeolitic material per ton of aluminum waste. Moreover, this zeolite synthesis route did not lead to the generation of solid residues. Liquid effluents, known as mother liquor and rinse water, can be completely recycled, consequently saving water. In addition, the gases generated in the process such as ammonia and hydrogen can be recovered as byproducts and used for other applications. This recovery represents an added value for the process.

The conversion of hazardous aluminum waste into zeolite can be considered a sustainable process, that can reduce the high environmental impact of waste and contribute to the circular economy.

Declaration of competing interest

The authors declare that they have no known competing financial interests or personal relationships that could have appeared to influence the work reported in this paper.

CRediT authorship contribution statement

Aurora López-Delgado: Conceptualization, Investigation, Methodology, Supervision, Writing - original draft. **José I. Robla:** Investigation, Writing - original draft. **Isabel Padilla:** Investigation, Formal analysis, Writing - review & editing. **Sol López-Andrés:** Writing - review & editing. **Maximina Romero:** Writing - review & editing.

Acknowledgments

The authors thank Recuperaciones y Reciclajes Roman S.L. (Madrid, Spain) for supplying the aluminum waste, Clemente Roman S.L. (Segovia, Spain) for the use of its facilities and Dr. Sánchez-Hernández for her invaluable help in the characterization of samples. The authors also thank MINECO (Ministry of Economy and Competitiveness) - Spain for its financial support (Project CTM2012-34449).

References

Álvarez-Ayuso, E., Garcıa-Sánchez, A., Querol, X., 2003. Purification of metal electroplating waste waters using zeolites. Water Res. 37 (20), 4855–4862.
Antrekowitsch, S.L., 2007. Hydrogen as a reducing agent: state-of-the-art science and technology. J. Occup. Med. 59 (6), 20–26.
Anuwattana, R., Khummongkol, P., 2009. Conventional hydrothermal synthesis of Na-A zeolite from cupola slag and aluminum sludge. J. Hazard Mater. 166 (1), 227–232.
Arenas, M.A., Padilla, I., Robla, J.I., Vázquez, A.J., López-Delgado, A., 2019. The use of concentrated solar energy for the reduction of CuO in H_2. Sol. Energy 180, 640–647.
Ayele, L., Pérez-Pariente, J., Chebude, Y., Díaz, I., 2015. Synthesis of zeolite A from Ethiopian kaolin. Microporous Mesoporous Mater. 215, 29–36.

Ayele, L., Pérez-Pariente, J., Chebude, Y., Díaz, I., 2016. Conventional versus alkali fusion synthesis of zeolite A from low grade kaolin. Appl. Clay Sci. 132–133, 485–490.

Baccouche, A., Srasra, E., El Maaoui, M., 1998. Preparation of Na-P1 and sodalite octahydrate zeolites from interstratified illite-smectite. Appl. Clay Sci. 13 (4), 255–273.

Bukhari, S.S., Behin, J., Kazemian, H., Rohani, S., 2015. Conversion of coal fly ash to zeolite utilizing microwave and ultrasound energies: a review. Fuel 140 (0), 250–266.

Cardoso, A.M., Horn, M.B., Ferret, L.S., Azevedo, C.M.N., Pires, M., 2015a. Integrated synthesis of zeolites 4A and Na–P1 using coal fly ash for application in the formulation of detergents and swine wastewater treatment. J. Hazard Mater. 287, 69–77.

Cardoso, A.M., Paprocki, A., Ferret, L.S., Azevedo, C.M.N., Pires, M., 2015. Synthesis of zeolite Na-P1 under mild conditions using Brazilian coal fly ash and its application in wastewater treatment. Fuel 139, 59–67..

Chareonpanich, M., Jullaphan, O., Tang, C., 2011. Bench-scale synthesis of zeolite A from subbituminous coal ashes with high crystalline silica content. J. Clean. Prod. 19 (1), 58–63.

Dimitrijevic, R., Dondur, V., Vulic, P., Markovic, S., Macura, S., 2004. Structural characterization of pure Na-nephelines synthesized by zeolite conversion route. J. Phys. Chem. Solid. 65 (10), 1623–1633.

European_Directive-2008/98/EC, 2008. Directive 2008/98/EC of the European parliament and of the Council of 19 november 2008 on waste and repealing certain Directives. Off. J. Eur. Union. L 312, 3–30.

Farag, I.H., Zhang, J., 2012. Simulation of Synthetic zeolites 4A and 5A manufacturing for green processing. Eng. Sci. Technol.: An. Int. J. 2 (2), 8.

Fawer, M., Postlethwaite, D., Klüppel, H.-J., 1998. Life cycle inventory for the production of zeolite a for detergents. Int. J. Life Cycle Assess. 3 (2), 71–74.

Flanigen, E.M., Khatami, H., Szymanski, H.A., 1974. Infrared structural studies of zeolite frameworks, molecular sieve zeolites-I. Am. Chem. Soc. 201–229.

Galindo, R., Padilla, I., Rodríguez, O., Sánchez-Hernández, R., López-Andrés, S., López-Delgado, A., 2015. Characterization of solid wastes from aluminum tertiary sector: the current state of Spanish industry. J. Miner. Mater. Char. Eng. 3 (02), 55.

Gautam, M., Pandey, D., Agrawal, S.B., Agrawal, M., 2016. Metals from mining and metallurgical industries and their toxicological impacts on plants. In: Singh, A., Prasad, S.M., Singh, R.P. (Eds.), Plant Responses to Xenobiotics. Springer Singapore, Singapore, pp. 231–272.

Hashemian, S., Hosseini, S.H., Salehifar, H., Salari, K., 2013. Adsorption of Fe(III) from aqueous solution by Linde type-A zeolite. Am. J. Anal. Chem. 4.

Hollman, G.G., Steenbruggen, G., Janssen-Jurkovičová, M., 1999. A two-step process for the synthesis of zeolites from coal fly ash. Fuel 78 (10), 1225–1230.

Huang, X.-L., Badawy, A.E., Arambewela, M., Ford, R., Barlaz, M., Tolaymat, T., 2014. Characterization of salt cake from secondary aluminum production. J. Hazard Mater. 273 (0), 192–199.

Huang, X.-L., El Badawy, A.M., Arambewela, M., Adkins, R., Tolaymat, T., 2015. Mineral phases and metals in baghouse dust from secondary aluminum production. Chemosphere 134, 25–30.

IAI (International Aluminium Institute), 2018. Statistics. http://www.world-aluminium.org/statistics/primary-aluminium-production/#data.

Ismail, A.A., Mohamed, R.M., Ibrahim, I.A., Kini, G., Koopman, B., 2010. Synthesis, optimization and characterization of zeolite A and its ion-exchange properties. Colloids Surf., A 366 (1), 80–87.

IZA, 2017. International zeolite association. http://europe.iza-structure.org/IZA-SC/material_tm.php?STC=LTA.

Johnson, E.B.G., Arshad, S.E., 2014. Hydrothermally synthesized zeolites based on kaolinite: a review. Appl. Clay Sci. 97–98, 215–221.

Kugbe, J., Matsue, N., Henmi, T., 2009. Synthesis of Linde type A zeolite–goethite nanocomposite as an adsorbent for cationic and anionic pollutants. J. Hazard Mater. 164 (2), 929–935.

López-Delgado, A., Tayibi, H., 2012. Can hazardous waste become a raw material? The case study of an aluminium residue: a review. Waste Manag. Res. 30 (5), 474–484.

López-Delgado, A., Padilla, I., Sánchez-Hernández, R., Rodríguez, O., López-Andrés, S., 2017. Procedimiento de revalorización de un residuo procedente de la molienda de escorias de aluminio, p. 40. Spanish Patent ES 2617037B1. Spain.

Mahinroosta, M., Allahverdi, A., 2018. Hazardous aluminum dross characterization and recycling strategies: a critical review. J. Environ. Manag. 223, 452–468.

Mallapur, Veeresh P., Oubagaranadin, J.U.L., 2017. A brief review on the synthesis of zeolites from hazardous wastes. Trans. Indian Ceram. Soc. 76 (1), 13.

Osoba, L.O., Owolabi, O.B., Talabi, S.I., Adeosun, S.O., 2018. Review on oxide formation and aluminum recovery mechanism during secondary smelting. J. Cast. Mater. Eng. 2 (2).

Querol, X., Umaña, J.C., Plana, F., Alastuey, A., Lopez-Soler, A., Medinaceli, A., Valero, A., Domingo, M.J., Garcia-Rojo, E., 2001. Synthesis of zeolites from fly ash at pilot plant scale. Examples of potential applications. Fuel 80 (6), 857–865.

Querol, X., Moreno, N., Umaa, J.C., Alastuey, A., Hernández, E., López-Soler, A., Plana, F., 2002. Synthesis of zeolites from coal fly ash: an overview. Int. J. Coal Geol. 50 (1–4), 413–423.

Radulović, A., Dondur, V., Vulić, P., Miladinović, Z., Ćirić-Marjanović, G., Dimitrijević, R., 2013. Routes of synthesis of nepheline-type polymorphs: an influence of Na-LTA bulk composition on its thermal transformations. J. Phys. Chem. Solid. 74 (9), 1212–1220.

Renda, A., Pelkmans, J., Egenhofer, C., Marcu, A., Schrefler, L., Luchetta, G., Simonelli, F., Genoese, F., Valiante, D., Mustilli, F., Colantoni, L., Infelise, F., Stoefs, W., Teusch, J., Timini, J., Wieczorkiewicz, J., Zavatta, R., Giannotti, E., Stecchi, G.M., 2013. Assessment of cumulative cost impact for the steel and the aluminium industry - final report aluminium. Assessment of cumulative cost impact for the steel and the aluminium industry - final report aluminium.

Sánchez-Hernández, R., 2018. Complete Transformtion of Alumium Waste into Zeolite and its Use in the Removal of Pollutans from Aqueous Solution. Ph D Tesis. University Carlos III of Madrid, Spain.

Sánchez-Hernández, R., López-Delgado, A., Padilla, I., Galindo, R., López-Andrés, S., 2016. One-step synthesis of NaP1, SOD and ANA from a hazardous aluminum solid waste. Microporous Mesoporous Mater. 226, 267–277.

Sánchez-Hernández, R., Padilla, I., López-Andres, S., López-Delgado, A., 2017. Eco-friendly bench-scale zeolitization of an Al-containing waste into gismondine-type zeolite under effluent recycling. J. Clean. Prod. 161, 792–802.

Sommerville, R., Blissett, R., Rowson, N., Blackburn, S., 2013. Producing a synthetic zeolite from improved fly ash residue. Int. J. Miner. Process. 124, 20–25.

Su, S., Ma, H., Chuan, X., 2016. Hydrothermal synthesis of zeolite A from K-feldspar and its crystallization mechanism. Adv. Powder Technol. 27 (1), 139–144.

Terzano, R., D'Alessandro, C., Spagnuolo, M., Romagnoli, M., Medici, L., 2015. Facile zeolite synthesis from municipal glass and aluminum solid wastes. Clean 43 (1), 133–140.

Volli, V., Purkait, M.K., 2015. Selective preparation of zeolite X and A from flyash and its use as catalyst for biodiesel production. J. Hazard Mater. 297, 101–111.

Wang, C.-F., Li, J.-S., Wang, L.-J., Sun, X.-Y., 2008. Influence of NaOH concentrations on synthesis of pure-form zeolite A from fly ash using two-stage method. J. Hazard Mater. 155 (1–2), 58–64.

Wang, P., Sun, Q., Zhang, Y., Cao, J., 2019. Synthesis of zeolite 4A from kaolin and its adsorption equilibrium of carbon dioxide. Materials 12 (9), 1536.

Wdowin, M., Franus, M., Panek, R., Badura, L., Franus, W., 2014. The conversion technology of fly ash into zeolites. Clean Technol. Environ. 16 (6), 1217–1223.

Xu, R., Pang, W., Yu, J., Huo, Q., Chen, J., 2007. Synthetic Chemistry of Microporous Compounds (I) – Fundamentals and Synthetic Routes, Chemistry of Zeolites and Related Porous Materials. John Wiley & Son, Pte LTD, pp. 117–189.

Yamukyan, M.H., Manukyan, K.V., Kharatyan, S.L., 2009. Copper oxide reduction by hydrogen under the self-propagation reaction mode. J. Alloys Compd. 473 (1–2), 546–549.

Yang, G.C.C., Yang, T.-Y., 1998. Synthesis of zeolites from municipal incinerator fly ash. J. Hazard Mater. 62 (1), 75–89.

Zhang, C., Li, S., 2018. Utilization of iron ore tailing for the synthesis of zeolite A by hydrothermal method. J. Mater. Cycles Waste Manag. 20 (3), 1605–1614.